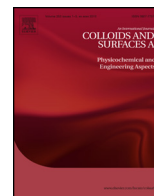




Contents lists available at ScienceDirect

Colloids and Surfaces A: Physicochemical and Engineering Aspects

journal homepage: www.elsevier.com/locate/colsurfa



Applications and extensions of the Z-cone model for the energy of a foam

David Whyte*, Robert Murtagh, Denis Weaire, Stefan Hutzler

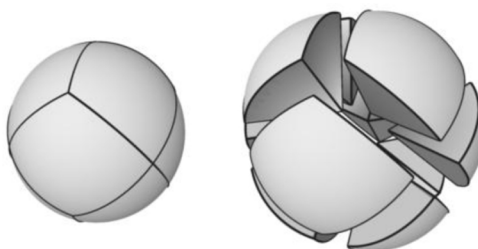
School of Physics, Trinity College Dublin, Dublin 2, Ireland

HIGHLIGHTS

- We compute an effective Hookean spring constant as a function of contact number for bubble–bubble interactions.
- We use the analytic Z-cone model to obtain a liquid fraction profile for a foam under gravity.
- We extend the Z-cone model to allow the computation of energies for bubbles of differing sizes.

GRAPHICAL ABSTRACT

A bubble in an ordered foam can be split into sections: one for each neighbour. We approximate these sections as spherical cones and obtain an analytic form for the energy as a function of deformation, and use this to obtain a liquid fraction profile for a foam under gravity.



ARTICLE INFO

Article history:
Received 6 November 2014
Received in revised form
19 December 2014
Accepted 20 December 2014
Available online xxx

Keywords:
Foams
Emulsions
Minimal surfaces

ABSTRACT

We present an extended analysis of the Z-cone model for the estimation of the energy of an ordered foam. In particular, we show that it results in an interaction potential with an exponent consistent with those previously reported, as well as an equilibrium liquid fraction profile under gravity consistent with those experimentally observed in ordered foams. We also extend the model to deal with curved interfaces, as a first step to modelling ordered bidisperse foams.

© 2015 Published by Elsevier B.V.

1. Introduction

Foams containing a high percentage of liquid (i.e., wet foams) play an important role in many industrial processes, such as foam fractionation [1] and enhanced oil recovery [2]. They continue to pose theoretical problems regarding the understanding of their surface energy, which determines many of their significant properties, including the structure itself. While the use of the Surface Evolver

software [3] has been successfully applied to both ordered and disordered dry foams [4], the simulation of wet foams by that method remains problematic, particularly in the case of disorder.

Representing bubbles in two-dimensional foams as soft overlapping disks has proved a powerful tool for understanding their behaviour [5–7]; however there is room for alternative approaches, particularly in three dimensions.

The recently developed Z-cone model [8] is analytically tractable, at least in the simple cases which we have so far considered, i.e., some monodisperse crystalline foams. The model proceeds from the decomposition of a bubble with Z neighbours into Z equivalent pieces (as shown in Fig. 1), followed by their approximation as

* Corresponding author. Tel.: +353 18961469
E-mail address: dawhyte@tcd.ie (D. Whyte).

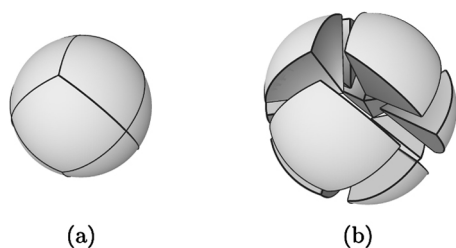


Fig. 1. A bubble in an fcc-ordered ($Z = 12$) foam can be divided up into 12 equivalent pieces: one for each neighbour. In the Z -cone model, each of these is approximated by a spherical cone whose cap is flattened by contact with a neighbouring bubble.

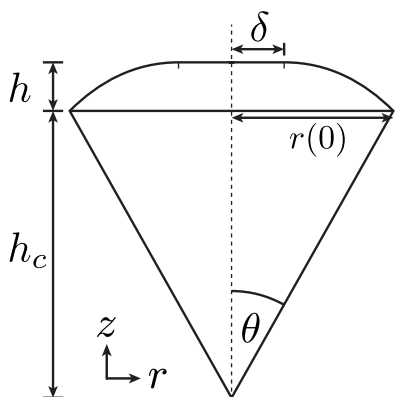


Fig. 2. A cross-section of one cone, showing several quantities which we use. The shape of the cap is defined by the function $r(z)$, and consists of a rim with a curvature related to Laplace pressure, and a flat centre, representing contact with a neighbour.

circular cones. Both liquid and gas are treated as incompressible, and we neglect all forces except for surface tension. The surface area of the cap of each cone is minimised under the constraint of volume conservation.

Previously [8] we used the model to compute analytical parametric expressions for energy as a function of deformation and liquid fraction consistent with those obtained from Surface Evolver simulations, as well as an expression for osmotic pressure. Furthermore, we discussed the logarithmic singularities in the wet foam limit.

In this paper we demonstrate further success of the model by the computation of liquid fraction profiles in good agreement with published experimental data. We also present first steps of the application of the model to bidisperse ordered foams based on our analytical treatment of bubbles confined between spherical boundaries. Finally, we provide a detailed appendix fleshing out the mathematical treatment of the model.

2. Mathematical framework

We wish to obtain a form for the *dimensionless excess energy* for a bubble in a foam, which we define as:

$$\varepsilon = \frac{A}{A_0} - 1, \quad (1)$$

where A is the total surface area of the bubble, and A_0 is the surface area of the undeformed spherical bubble. In terms of the radius R of the undeformed bubble, we have $A_0 = 4\pi R^2$.

The primary results of the model are analytic expressions relating ε to the deformation ξ , defined as:

$$\xi = 1 - \frac{h + h_c}{R} \quad (2)$$

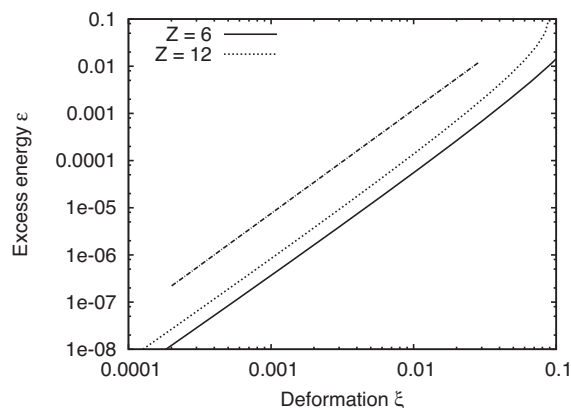


Fig. 3. Dependence of excess energy on deformation for $Z=6$ and 12, shown on a log-log plot. A line of slope 2.2 is shown as a guide to the eye, showing that $\varepsilon \propto \xi^{2.2}$ is a good approximation over a wide range of ξ .

where h and h_c are as shown in Fig. 2. $\xi = 0$ corresponds to an undeformed spherical bubble.

As described in Section 1, we aim to minimise the surface area of the cap of a spherical cone. We do so by the Euler–Lagrange method, subject to the appropriate constraints:

- The bubble volume, and hence the cone volume, remains constant.
- $\frac{dr}{dz} = \cot \theta$ at $z=0$: i.e., the bubble surface meets the edge of the cone at right angles.
- $\frac{dr}{dz} = \infty$ at $z=h$: i.e., the curved part of the cap meets the flat part smoothly.

This minimisation (which is presented fully in Appendix A) results in analytic expressions for ξ and ε in terms of the cap radius δ as shown in Fig. 2, in the form of elliptic integrals. Previously, we demonstrated the accuracy of these expressions by comparing them to the results of Surface Evolver simulations of bubbles with 6 and 12 neighbours in various arrangements [8].

Furthermore, simple geometrical considerations yield expressions for the liquid fraction $\phi(\xi, Z)$ and the critical liquid fraction ϕ_c , valid under the approximation of rotational symmetry:

$$\phi = 1 - \frac{1 - \phi_c}{(1 - \xi)^3}, \quad \phi_c = \frac{3 - 4/Z}{Z - 1}, \quad (3)$$

where ϕ_c is the critical liquid fraction: the liquid fraction at the wet limit. Hence, from our result for $\varepsilon(\xi)$ – (A.25) and (A.28) – we can now obtain a form for $\varepsilon(\phi)$ for any contact number Z .

3. Computation of effective spring constant for bubble–bubble interaction

It is well established that bubble–bubble interactions deviate from a simple harmonic force law [9]. For small values of deformation there is a logarithmic correction. For higher values the interaction may be roughly described as $\varepsilon \propto \xi^\alpha$, based on results of Surface Evolver simulations [10].

Fig. 3 shows, on a log-log plot, the variation of ε with ξ as obtained from the Z -cone model for $Z=6$ and 12, showing that $\alpha \approx 2.2$ is satisfactory for a wide range of ξ . This is broadly in line with results obtained by Lacasse et al. [10], and represents an interaction which lies between the harmonic case: Hooke's law, i.e., $\alpha = 2$, and the so-called Hertzian case with $\alpha = 2.5$.

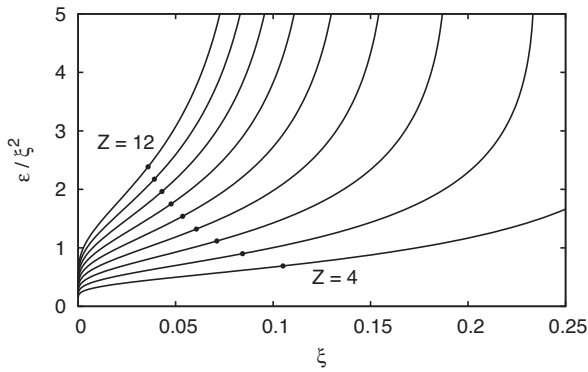


Fig. 4. We use the point at which ε/ξ^2 has least slope as a function of ξ to obtain an effective Hooke's law constant k_{eff} for each value of Z . k_{eff} increases with Z .

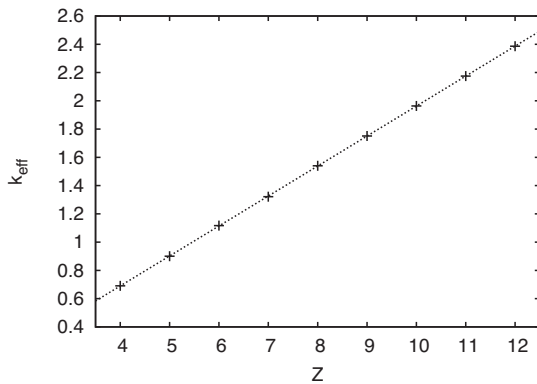


Fig. 5. The variation of the effective spring constant k_{eff} with the number of contacts Z is well described by the linear relationship (5).

Hence we cannot accurately refer to a spring constant k , but we may define an effective spring constant k_{eff} :

$$k_{\text{eff}} = \left. \frac{\varepsilon}{\xi^2} \right|_{\xi=\xi_{\text{inf}}} \quad (4)$$

where ξ_{inf} is the inflection point on the plot of ε/ξ^2 : see Fig. 4. This inflection point represents the value of ξ at which ε/ξ^2 is 'flattest': this might reasonably be considered the point at which the approximation of harmonicity is best, since in the harmonic case $\varepsilon/\xi^2 = k$ for all ξ .

In Fig. 5 we plot the variation of k_{eff} with the number of contacts Z . We see a relationship which is very close to linear, with the line of best fit:

$$k_{\text{eff}} = 0.21(Z - 0.75). \quad (5)$$

While clearly an approximation, a local force law of the form $F = k_{\text{eff}}\xi$ is worth considering in any extensions of Durian's two-dimensional model [5] to three dimensions.

4. Liquid fraction profile

We can use the analytic predictions of the Z-cone model to compute a liquid fraction profile for a foam at equilibrium under gravity. We plot the obtained profile as a function of the dimensionless reduced height in Fig. 6, comparing it to a simple approximation from [11] and an empirical fit to experimental data for monodisperse ordered foams from [12].

The liquid fraction profile for the Z-cone model was derived by considering the osmotic pressure of the foam, which can be related directly to the variation of excess energy with liquid fraction. The concept of an osmotic pressure in a foam was first introduced by

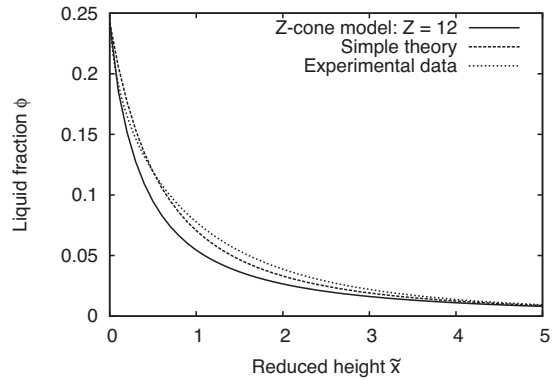


Fig. 6. The liquid fraction as a function of reduced height, obtained using the Z-cone model with $Z = 12$, compared to a simple theoretical expression from [11], and to an empirical expression obtained from experiments on monodisperse foams by [12]. The Z-cone model gives an adequate approximation of the experimental data in the wet limit.

Princen [13,14]. In the case where gas and liquid are treated as incompressible, Π is given by

$$\Pi = -\gamma \left(\frac{\partial S}{\partial V} \right)_{V_{\text{gas}}=\text{const.}}, \quad (6)$$

where S is the total surface area of the bubbles within a volume V , and γ is the surface tension of the liquid phase [15].

Physically, the osmotic pressure is simply the force per unit area on a semi-permeable membrane pressing on the foam, and is due to the fact that removing liquid from a foam deforms the bubbles, increasing their surface area.

We can relate the osmotic pressure to the excess energy ε (1) by

$$\tilde{\Pi} = -3(1 - \phi)^2 \frac{\partial \varepsilon}{\partial \phi}, \quad (7)$$

where $\tilde{\Pi}$ is the reduced osmotic pressure; $\tilde{\Pi} = \Pi/(\gamma/R)$.

The osmotic pressure is related to the local liquid fraction [13,15] by

$$d\tilde{\Pi} = (1 - \phi(\tilde{x})) d\tilde{x} \quad (8)$$

where we have introduced the reduced height $\tilde{x} = xR/l_0^2$, with l_0 being the capillary length for the foam, defined as $\sqrt{\gamma/(\rho g)}$. This relationship is obtained by balancing the osmotic pressure with the buoyancy force acting on bubbles.

Expanding (8) into partial derivatives, we obtain a differential equation for $\phi(\tilde{x})$ which depends on $\partial\tilde{\Pi}/\partial\phi$:

$$\frac{\partial \phi}{\partial \tilde{x}} = \frac{1 - \phi(\tilde{x})}{\partial\tilde{\Pi}/\partial\phi}, \quad \text{with } \phi(0) = \phi_c. \quad (9)$$

We can use (3) to obtain an expression for $\varepsilon(\phi)$ which we use with (7) to solve this differential equation numerically, yielding a liquid fraction profile for any Z . We choose $Z = 12$, as for fcc-ordered foams, and so (3) gives a critical liquid fraction $\phi_c = 0.242$. We plot the obtained liquid fraction in Fig. 6, and compare it to an empirical fit to experimentally measured profiles for monodisperse highly ordered foams from [12]. Note that the experimental data has a critical liquid fraction of 0.26.

While there is good agreement between the Z-cone model with $Z = 12$ and the experimental data in the wet limit, there is a discrepancy at lower ϕ . One possible source of this is the fact that $Z = 12$ does not hold throughout an ordered foam. When $\phi < 0.07$, bubbles tend to arrange in a Kelvin (bcc) structure more readily than fcc [15]. A bubble in such an arrangement does not have neighbours which are mutually equivalent and so our model does not strictly

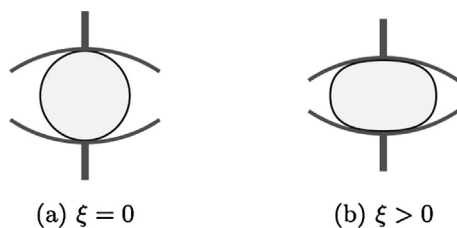


Fig. 7. We investigate the case of $Z=2$ contacts by using spherical boundaries, appropriate when the pressure of neighbouring bubbles is different from that of the central one.

apply in this case; however an effective $Z \approx 10.5$ gives reasonably accurate forms for ε [8].

In the same figure we have also plotted an expression for $\phi(\bar{x})$ following from [11], derived independently to the Z -cone model:

$$\phi(\bar{x}) = \tilde{c} \left(\bar{x} + \sqrt{\frac{\tilde{c}}{\phi_c}} \right)^{-2} \quad (10)$$

The derivation of this expression considers the vertical variation in cross-section of a Plateau border, based on the hydrostatic pressure variation in the liquid; together with a structural constant $\tilde{c} \approx 0.333$ related to the number of Plateau borders per volume in a Kelvin foam. The resulting Eq. (10), presented in this form for the first time, is a surprisingly good description of the experimental data, and has an appealingly simple form.

5. Extension of model to curved interfaces

Previously we derived analytic forms for ε and ξ for a monodisperse foam in which all bubbles are equivalent: in this case, the approximation of rotational symmetry implies a planar interface between neighbouring bubbles, since the internal pressure is the same for all bubbles. Here we extend the model to deal with the case of bubbles with differing pressures: under our approximation of rotational symmetry, the interface is a spherical cap. The radius of curvature R_c of the spherical cap can be obtained from the Laplace pressure difference ΔP between the bubbles:

$$R_c = \frac{4\gamma}{\Delta P} \quad (11)$$

Hence, when a bubble is smaller than its neighbours (and therefore has greater pressure) the interface curves outwards.

We have extended the Z -cone model to deal with such curved interfaces: the full treatment is given in Appendix A, and we arrive at somewhat lengthy analytic expressions for both ξ and ε . There is a potential ambiguity in how we measure $h+h_c$ when we extend (2) – the definition of ξ – to curved interfaces. Here we define $h+h_c$ as the distance from the apex of the cone to its surface as measured along its axis of symmetry: the dashed line in Fig. 2.

Previously, we represented the presence of equal-sized neighbouring bubbles as flat plates compressing a bubble from each of Z directions. Here, we simulate a bubble confined between plates which are spherical caps: see Fig. 7. To prevent instability in the case where the plates curve inwards, fourfold symmetry was imposed around the vertical axis.

In Fig. 8 we compare the results of Surface Evolver simulations for $Z=2$ with the Z -cone model expressions for the excess energy as a function of deformation. The model is exact for the case of a flat interface, and accurately predicts the variation of energy over a wide range of deformations for both the convex ($R_c > 0$) and concave ($R_c < 0$) cases. The shallower increase in excess energy for the concave bubble is due to our choice of the definition of deformation ξ .

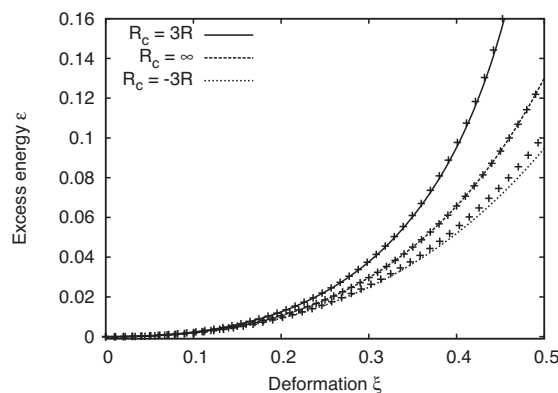


Fig. 8. For a bubble with two contacts, we compare the analytic expressions for the excess energy to the results of Surface Evolver simulations. For the case of a flat interface (radius of curvature $R_c \rightarrow \infty$) there is exact agreement between theory and simulation, to within numerical error. The analytic approximations for curved interfaces are good over a wide range of deformations ξ : the relative error increases with deformation, with a maximum of $\sim 8\%$ for $R_c = -3R$ and $\sim 3\%$ for $R_c = 3R$.

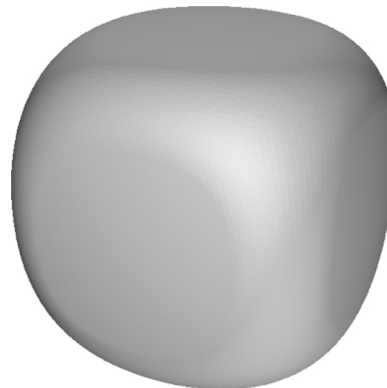


Fig. 9. Surface Evolver simulation of a bubble with $Z=6$ near the dry limit. The bubble is compressed between six plates arranged in a cube. Here, the plates are spherical caps with $R_c = 3R$, so the bubble bulges outwards.

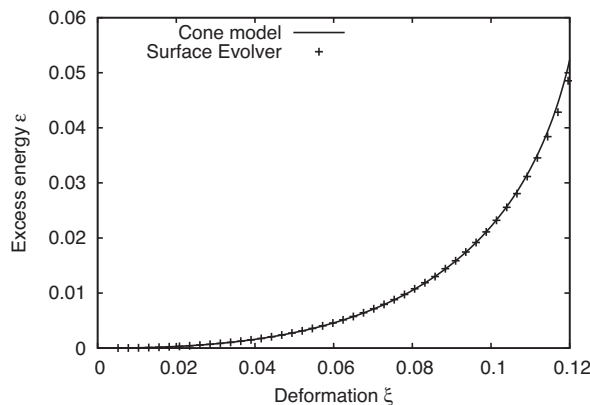


Fig. 10. The results of the simulation shown in Fig. 9 compared to the analytic predictions of the Z -cone model for $Z=6$. We see excellent agreement over a wide range of deformations ξ : the relative error does not exceed 5%.

Fig. 9 depicts a Surface Evolver simulation of a bubble with $Z=6$, and with higher pressure than its neighbours, so $R_c > 0$: the interfaces curve outwards. In Fig. 10, we compare the results of this simulation to the Z -cone model expressions, observing very good agreement between analytics and simulation.

6. Outlook

Previously we applied the Z-cone model to ordered monodisperse foams, requiring Z identical cones, with flat interfaces between bubbles in contact. Here we discussed Z identical cones with curved interfaces: this is a step towards understanding bidisperse foams – in particular, an arrangement such as the rocksalt structure in which each small ion is surrounded by six larger ones, and vice versa. A further extension would be the treatment of cells whose faces are not all equivalent (such as the Kelvin cell): this requires careful treatment of a set of cones whose solid angles and volumes are not all equal.

Acknowledgements

This publication has emanated from research supported in part by a research grant from Science Foundation Ireland (SFI) under grant number 13/IA/1926. The work was co-funded by the European Regional Development Fund and the HEA, Ireland. We also wish to acknowledge COST actions MP1106: Smart and Green Interfaces and MP1305: Flowing Matter. We would like to thank R. Höhler for discussions about wet foams.

Denis Weaire acknowledges a Gladden Fellowship of the University of Western Australia during which part of this work was carried out.

We thank the anonymous referees for their help in clarifying the manuscript.

Appendix A. Mathematics of the cone model for monodisperse foam with Z identical neighbours

The total surface area per contact Z, A_Z, of our bubble can be written as

$$A_Z = A_f + 2\pi \int_0^h r(z) \sqrt{1 + \left(\frac{dr(z)}{dz}\right)^2} dz, \tag{A.1}$$

where A_f is the surface area of the contact. In the case of flat contacts A_f = πδ². The second term in this equation is the general expression for the surface area (of revolution) of any curve given by r(z). The volume under this curve is given by

$$V_Z = \pi \int_0^h r(z)^2 dz + \frac{\pi r(0)^3 \cot \theta}{3}. \tag{A.2}$$

Minimising this surface area under the constraint of constant volume requires the Euler–Lagrange formalism. In general, the Euler–Lagrange equation is given by

$$\frac{dL\left(r(z), \frac{dr(z)}{dz}, z\right)}{dr(z)} - \frac{d}{dz} \frac{dL\left(r(z), \frac{dr(z)}{dz}, z\right)}{d\left(\frac{dr(z)}{dz}\right)} = 0. \tag{A.3}$$

The Lagrangian function L that we consider does not depend explicitly on the coordinate z

$$L\left(r(z), \frac{dr(z)}{dz}\right) = 2r(z) \sqrt{1 + \left(\frac{dr(z)}{dz}\right)^2} - \lambda r(z)^2. \tag{A.4}$$

In this special case, we can make a significant simplification of our minimisation problem by using an integrated form of the Euler–Lagrange Eq. (A.5) whose derivation we give here

$$\begin{aligned} \int \frac{dL}{dr(z)} dr(z) - \int \frac{d}{dz} \frac{dL}{d\left(\frac{dr(z)}{dz}\right)} dz &= \int 0 dr(z), \\ C + L - \int \frac{d}{dz} \left(\frac{dL}{d\left(\frac{dr(z)}{dz}\right)} \right) dz &= 0, \\ L - \int \frac{d}{dr(z)} \left(\frac{dr(z)}{dz} \left(\frac{dL}{d\left(\frac{dr(z)}{dz}\right)} \right) \right) dz &= -C, \\ L - \int d \left(\frac{dr(z)}{dz} \left(\frac{dL}{d\left(\frac{dr(z)}{dz}\right)} \right) \right) &= -C, \\ \therefore \frac{dr(z)}{dz} \frac{dL}{d\left(\frac{dr(z)}{dz}\right)} - L &= C, \end{aligned} \tag{A.5}$$

where C is an unknown integration constant.

Inserting our Lagrangian function and its derivative into the integrated Euler–Lagrange equation we obtain

$$-\frac{2r(z)}{\sqrt{1 + \left(\frac{dr(z)}{dz}\right)^2}} + \lambda r(z)^2 = C. \tag{A.6}$$

The unknown constants λ and C are determined by imposing the following boundary conditions on the equation:

$$\left. \frac{dr(z)}{dz} \right|_{z=h} = \infty \tag{A.7}$$

$$\left. \frac{dr(z)}{dz} \right|_{z=0} = \cot \theta. \tag{A.8}$$

The first of these ensures that the bubble surface meets the flat contact smoothly while the second ensures that the bubble surface meets the cone at a right angle. By splitting the 4π steradian solid angle of our bubble equally between each contact we can write

$$\theta = \arccos \left(1 - \frac{2}{Z} \right). \tag{A.9}$$

Using these conditions in Eq. (A.6) we have, after some algebra, that

$$\Rightarrow \frac{r(z)}{\sqrt{1 + \left(\frac{dr(z)}{dz}\right)^2}} = \frac{r(0)(r(z)^2 - \delta^2)}{(r(0)^2 - \delta^2) \sqrt{1 + \frac{(z-2)^2}{4(z-1)}}}. \tag{A.10}$$

Rescaling this equation in terms of the dimensionless quantities ρ(z) = r(z)/r(0) and ρ_δ = δ/r(0) yields

$$\Rightarrow \sqrt{1 + \left(\frac{dr(z)}{dz}\right)^2} = \frac{\rho(z) \frac{z}{2\sqrt{z-1}} (1 - \rho_\delta^2)}{\rho(z)^2 - \rho_\delta^2}. \tag{A.11}$$

This is a dimensionless first-order differential equation which can be solved by integrating it between the limits of ρ_δ and ρ(z). Rearranging this equation for dz and noting that dr(z) = r(0) dρ(z), we find that

$$\int_{-h}^z dz = z + h = r(0) I(\rho(z), \rho_\delta, Z) \tag{A.12}$$

and so

$$z = -h + r(0) I(\rho(z), \rho_\delta, Z). \tag{A.13}$$

where I(ρ(z), ρ_δ, Z) is a definite elliptic integral defined below.

By considering $\rho(z=0) = 1$ in Eq. (A.13), we obtain the important identity

$$r(0) = \frac{h}{I_\delta(\rho_\delta, Z)}, \quad (\text{A.14})$$

allowing us to express the bubble profile as

$$z(\rho(z), \rho_\delta, Z) = h \left[\frac{I(\rho(z), \rho_\delta, Z)}{I_\delta(\rho_\delta, Z)} - 1 \right]. \quad (\text{A.15})$$

The elliptic integrals $I(\rho(z), \rho_\delta, Z)$ and $I_\delta(\rho_\delta, Z)$, which need to be evaluated numerically, are given by

$$I(\rho(z), \rho_\delta, Z) = \int_{\rho_\delta}^{\rho(z)} (x^2 - \rho_\delta^2) f(x, \rho_\delta, Z) dx \quad (\text{A.16})$$

and

$$I_\delta(\rho_\delta, Z) = \int_{\rho_\delta}^1 (x^2 - \rho_\delta^2) f(x, \rho_\delta, Z) dx, \quad (\text{A.17})$$

with

$$f(x, \rho_\delta, Z) = \left[\frac{Z^2}{4(Z-1)} x^2 (1 - \rho_\delta^2)^2 - (x^2 - \rho_\delta^2)^2 \right]^{-\frac{1}{2}}. \quad (\text{A.18})$$

The volume V_Z of our single cone is equal to $1/Z$ of the volume of a spherical bubble so that $V_Z = 4\pi R^3/3 Z$. Inserting this expression into Eq. (A.2) and solving for $r(0)$ yields

$$r(0) = \frac{h}{I_\delta(\rho_\delta, Z)} = R \left[\frac{\left(\frac{4}{Z}\right)}{3J_\delta(\rho_\delta, Z) + \frac{Z-2}{2\sqrt{Z-1}}} \right]^{\frac{1}{3}} \quad (\text{A.19})$$

where $J_\delta(\rho_\delta, Z)$ is another elliptic integral given by

$$J_\delta(\rho_\delta, Z) = \int_{\rho_\delta}^1 x^2 (x^2 - \rho_\delta^2) f(x, \rho_\delta, Z) dx. \quad (\text{A.20})$$

Eq. (A.19) reduces to $R \sin \theta$, the familiar case of a simple cone, in the limit as $\rho_\delta \rightarrow 0$. The constraint of volume conservation intuitively requires $r(0)$ (and hence h_c) to increase with increasing deformation to counteract the decrease in the height h .

Making use of Eqs. (A.11), (A.12) and (A.19), we can re-express the surface area per contact A_Z as

$$A(\rho_\delta, Z) = \pi R^2 \left(\frac{\left(\frac{4}{Z}\right)}{3J_\delta(\rho_\delta, Z) + \frac{Z-2}{2\sqrt{Z-1}}} \right)^{\frac{2}{3}} \left[\rho_\delta^2 + \frac{Z}{\sqrt{Z-1}} (1 - \rho_\delta^2) K_\delta(\rho_\delta, Z) \right] \quad (\text{A.21})$$

where $K_\delta(\rho_\delta, Z)$ is further elliptic integral given by

$$\varepsilon(\rho_\delta, Z) = \frac{A_Z(\rho_\delta, Z)}{A_{Z0}(Z)} - 1 \quad (\text{A.23})$$

The dimensionless excess surface energy is defined as

$$\varepsilon(\rho_\delta, Z) = \frac{A(\rho_\delta, Z)}{A_0(Z)} - 1 \quad (\text{A.23})$$

where $A_{Z0}(Z)$ is the surface area of the top of a spherical sector corresponding to our undeformed cone. From simple geometry, this is

$$A_{Z0}(Z) = 2\pi R^2 (1 - \cos \theta) = \frac{4\pi R^2}{Z}. \quad (\text{A.24})$$

Combining Z of these spherical sectors recovers the total surface area of a spherical bubble of $4\pi R^2$, as expected.

Therefore, the dimensionless excess energy is

$$\varepsilon(\rho_\delta, Z) = \frac{\rho_\delta^2 + \frac{Z}{\sqrt{Z-1}} (1 - \rho_\delta^2) K_\delta(\rho_\delta, Z)}{Z^{-\frac{1}{3}} \left(6J_\delta(\rho_\delta, Z) + \frac{Z-2}{\sqrt{Z-1}} \right)^{\frac{2}{3}}} - 1 \quad (\text{A.25})$$

The dimensionless deformation is defined, to the middle of the flat contact, as

$$\xi = 1 - \frac{h + h_c}{R} \quad (\text{A.26})$$

where the height of a cone h_c is given by

$$h_c = r(0) \frac{Z-2}{2\sqrt{Z-1}}. \quad (\text{A.27})$$

Using Eq. (A.19), this dimensionless deformation is

$$\xi(\rho_\delta, Z) = 1 - \left(\frac{\left(\frac{4}{Z}\right)}{3J_\delta(\rho_\delta, Z) + \frac{Z-2}{2\sqrt{Z-1}}} \right)^{\frac{1}{3}} \left[\frac{Z-2}{2\sqrt{Z-1}} + I_\delta(\rho_\delta, Z) \right]. \quad (\text{A.28})$$

The plots of dimensionless excess energy as a function of dimensionless deformation, for each value of Z , are produced by plotting Eqs. (A.25) and (A.28) parametrically as a function of ρ_δ .

Appendix B. Curved contact model

The purpose of this section is to provide sufficient analytical expressions to reproduce the figures provided in the main paper for the Z-Cone Model with curved contacts for both the relatively small and relatively large bubbles. The derivation of the following expressions is similar to that given above for the Z-Cone Model with flat contacts.

Beginning with the smaller of the contacting bubbles, the radius of our neighbouring bubbles R_n can be written as $R_n = aR$ with $a > 1$. Our cone has a smaller radius than its neighbour, meaning a higher Laplace pressure and, hence, the interfaces between the bubbles are curved “out” as shown in Fig. 7. The radius of curvature R_c of the interfaces between the bubbles is obtained from the difference in Laplace pressures of the undeformed bubbles. The introduction of curved interfaces introduces two new angles θ_{\min} and α into our model. The angle θ_{\min} corresponds to the angle made between the axis of symmetry and a line from the edge of the curved contact to the apex of the cone. The angle α corresponds to the angle made at the edge of the curved contact between the contact and a plane perpendicular to the axis of symmetry.

For each Z and a , there are unique values of θ_{\min} and α obtained by numerically solving

$$\widehat{I}_\delta(\rho_\delta, \theta_{\min}, Z) = \frac{\rho_\delta}{\tan \theta_{\min}} - \frac{Z-2}{2\sqrt{Z-1}} \quad (\text{B.1})$$

and

$$\sin \alpha = \rho_\delta \left(\frac{a-1}{a} \right) \left[\frac{\left(\frac{4}{Z}\right) - \left(\frac{a}{a-1}\right)^3 (2 - 3 \cos \alpha + \cos^3 \alpha)}{3\widehat{J}_\delta(\rho_\delta, \theta_{\min}, Z) + \frac{Z-2}{2\sqrt{Z-1}}} \right]^{\frac{1}{3}}. \quad (\text{B.2})$$

The dimensionless excess energy for the small bubble $\varepsilon(\rho_\delta, \theta_{\min}, \alpha, Z, a)$ is written as

$$\begin{aligned} \varepsilon(\rho_\delta, \theta_{\min}, \alpha, Z, a) &= \frac{Z}{4} \left(\frac{\left(\frac{4}{Z}\right) - \left(\frac{a}{a-1}\right)^3 (2 - 3 \cos \alpha + \cos^3 \alpha)}{3\widehat{J}_\delta(\rho_\delta, \theta_{\min}, Z) + \frac{Z-2}{2\sqrt{Z-1}}} \right)^{\frac{2}{3}} \\ &\times \left[\rho_\delta^2 + \left(\frac{a}{a-1}\right)^2 (1 - \cos \alpha)^2 \left(\frac{\left(\frac{4}{Z}\right) - \left(\frac{a}{a-1}\right)^3 (2 - 3 \cos \alpha + \cos^3 \alpha)}{3\widehat{J}_\delta(\rho_\delta, \theta_{\min}, Z) + \frac{Z-2}{2\sqrt{Z-1}}} \right)^{-\frac{2}{3}} \right. \\ &\left. + \frac{Z}{\sqrt{Z-1}} (1 - \rho_\delta^2) \widehat{K}_\delta(\rho_\delta, \theta_{\min}, Z) \right] - 1. \quad (\text{B.3}) \end{aligned}$$

The dimensionless deformation for the small bubble $\xi(\rho_\delta, \theta_{\min}, \alpha, Z, a)$, measured to the middle of the curved contact, is expressed as

$$\xi(\rho_\delta, \theta_{\min}, \alpha, Z, a) = 1 - \left(\frac{\left(\frac{4}{Z}\right) - \left(\frac{a}{a-1}\right)^3 (2 - 3 \cos \alpha + \cos^3 \alpha)}{3\widehat{J}_\delta(\rho_\delta, \theta_{\min}, Z) + \frac{Z-2}{2\sqrt{Z-1}}} \right)^{\frac{1}{3}} \times \left[\frac{Z-2}{2\sqrt{Z-1}} + \widehat{I}_\delta(\rho_\delta, \theta_{\min}, Z) \right] - \left(\frac{a}{a-1}\right) (1 - \cos \alpha). \quad (\text{B.4})$$

The definite elliptic integrals $\widehat{I}_\delta(\rho_\delta, \theta_{\min}, Z)$, $\widehat{J}_\delta(\rho_\delta, \theta_{\min}, Z)$ and $\widehat{K}_\delta(\rho_\delta, \theta_{\min}, Z)$ are given by:

$$\widehat{I}_\delta(\rho_\delta, \theta_{\min}, Z) = \int_{\rho_\delta}^1 \left[(x^2 - \rho_\delta^2) - \rho_\delta \sin \theta_{\min} \frac{Z}{2\sqrt{Z-1}} (x^2 - 1) \right] \widehat{f}(x, \rho_\delta, \theta_{\min}, Z) dx, \quad (\text{B.5})$$

$$\widehat{J}_\delta(\rho_\delta, \theta_{\min}, Z) = \int_{\rho_\delta}^1 x^2 \left[(x^2 - \rho_\delta^2) - \rho_\delta \sin \theta_{\min} \frac{Z}{2\sqrt{Z-1}} (x^2 - 1) \right] \widehat{f}(x, \rho_\delta, \theta_{\min}, Z) dx, \quad (\text{B.6})$$

$$\widehat{K}_\delta(\rho_\delta, \theta_{\min}, Z) = \int_{\rho_\delta}^1 x^2 \widehat{f}(x, \rho_\delta, \theta_{\min}, Z) dx, \quad (\text{B.7})$$

with

$$\widehat{f}(x, \rho_\delta, \theta_{\min}, Z) = \left[\frac{Z^2}{4(Z-1)} x^2 (1 - \rho_\delta^2)^2 - \left[(x^2 - \rho_\delta^2) - \rho_\delta \sin \theta_{\min} \frac{Z}{2\sqrt{Z-1}} (x^2 - 1) \right]^2 \right]^{-\frac{1}{2}}. \quad (\text{B.8})$$

For the large bubble we need to determine the dimensionless ratios ρ_{\min} and ρ_{\max} by numerically solving

$$\rho_{\min} = (a-1)^{-1} \sin \alpha \left(\frac{\left(\frac{4}{Z}\right) + (a-1)^{-3} (2 - 3 \cos \alpha + \cos^3 \alpha)}{3\widetilde{J}_\delta(\rho_{\max}, Z) + \widetilde{J}_\delta(\rho_{\min}, \rho_{\max}, \theta_{\min}, Z) + \frac{Z-2}{2\sqrt{Z-1}}} \right)^{-\frac{1}{3}} \quad (\text{B.9})$$

for the paired values of ρ_{\min} and ρ_{\max} which give the smallest excess energy provided $\rho_{\min} < \rho_\delta$ and $\rho_{\min} < \rho_{\max}$.

The dimensionless excess energy for the large bubble $\varepsilon(\rho_{\min}, \rho_{\max}, \theta_{\min}, \alpha, Z, a)$ is written as

$$\begin{aligned} \varepsilon(\rho_{\min}, \rho_{\max}, \theta_{\min}, \alpha, Z, a) &= \frac{Z}{4} \left(\frac{\left(\frac{4}{Z}\right) + (a-1)^{-3} (2 - 3 \cos \alpha + \cos^3 \alpha)}{3\widetilde{J}_\delta(\rho_{\max}, Z) + \widetilde{J}_\delta(\rho_{\min}, \rho_{\max}, \theta_{\min}, Z) + \frac{Z-2}{2\sqrt{Z-1}}} \right)^{\frac{2}{3}} \\ &\quad \left[\rho_{\min}^2 + (a-1)^{-2} \left(\frac{\left(\frac{4}{Z}\right) + (a-1)^{-3} (2 - 3 \cos \alpha + \cos^3 \alpha)}{3\widetilde{J}_\delta(\rho_{\max}, Z) + \widetilde{J}_\delta(\rho_{\min}, \rho_{\max}, \theta_{\min}, Z) + \frac{Z-2}{2\sqrt{Z-1}}} \right)^{-\frac{2}{3}} \right. \\ &\quad \times (1 - \cos \alpha)^2 + 2(\rho_{\max}^2 - \rho_{\min}^2) \widetilde{K}_\delta(\rho_{\min}, \rho_{\max}, \theta_{\min}, Z) \\ &\quad \left. + \frac{Z}{\sqrt{Z-1}} (1 - \rho_{\max}^2) \widetilde{K}_\delta(\rho_{\max}, Z) \right] - 1. \quad (\text{B.10}) \end{aligned}$$

The dimensionless deformation for the small bubble $\xi(\rho_{\min}, \rho_{\max}, \theta_{\min}, \alpha, Z, a)$, again measured to the middle of the curved contact, is expressed as

$$\begin{aligned} \xi(\rho_{\min}, \rho_{\max}, \theta_{\min}, \alpha, Z, a) &= 1 + \frac{1 - \cos \alpha}{a-1} \\ &\quad - \left(\frac{\left(\frac{4}{Z}\right) + (a-1)^{-3} (2 - 3 \cos \alpha + \cos^3 \alpha)}{3\widetilde{J}_\delta(\rho_{\max}, Z) + \widetilde{J}_\delta(\rho_{\min}, \rho_{\max}, \theta_{\min}, Z) + \frac{Z-2}{2\sqrt{Z-1}}} \right)^{\frac{1}{3}} \\ &\quad \times \left[\frac{Z-2}{2\sqrt{Z-1}} + \widetilde{I}_\delta(\rho_{\min}, \rho_{\max}, \theta_{\min}, Z) + \widetilde{I}_\delta(\rho_{\max}, Z) \right]. \quad (\text{B.11}) \end{aligned}$$

The definite elliptic integrals defined for the large bubble are given by

$$\widetilde{I}_\delta(\rho_{\min}, \rho_{\max}, \theta_{\min}, Z) = \int_{\rho_{\min}}^{\rho_{\max}} \sin \theta_{\min} \rho_{\min} (x^2 - \rho_{\max}^2) \widetilde{f}(x, \rho_{\min}, \rho_{\max}, \theta_{\min}, Z) dx, \quad (\text{B.12})$$

$$\begin{aligned} \widetilde{J}_\delta(\rho_{\min}, \rho_{\max}, \theta_{\min}, Z) &= \int_{\rho_{\min}}^{\rho_{\max}} \sin \theta_{\min} \rho_{\min} x^2 (x^2 - \rho_{\max}^2) \\ &\quad \times \widetilde{f}(x, \rho_{\min}, \rho_{\max}, \theta_{\min}, Z) dx, \quad (\text{B.13}) \end{aligned}$$

$$\widetilde{K}_\delta(\rho_{\min}, \rho_{\max}, \theta_{\min}, Z) = \int_{\rho_{\min}}^{\rho_{\max}} x^2 \widetilde{f}(x, \rho_{\min}, \rho_{\max}, \theta_{\min}, Z) dx, \quad (\text{B.14})$$

$$\widetilde{I}_\delta(\rho_{\max}, Z) = \int_{\rho_{\max}}^1 (x^2 - \rho_{\max}^2) \widetilde{f}(x, \rho_{\max}, Z) dx, \quad (\text{B.15})$$

$$\widetilde{J}_\delta(\rho_{\max}, Z) = \int_{\rho_{\max}}^1 x^2 (x^2 - \rho_{\max}^2) \widetilde{f}(x, \rho_{\max}, Z) dx, \quad (\text{B.16})$$

$$\widetilde{K}_\delta(\rho_{\max}, Z) = \int_{\rho_{\max}}^1 x^2 \widetilde{f}(x, \rho_{\max}, Z) dx, \quad (\text{B.17})$$

with

$$\widetilde{f}(x, \rho_{\min}, \rho_{\max}, \theta_{\min}, Z) = \left[x^2 (\rho_{\min}^2 - \rho_{\max}^2)^2 - \sin^2 \theta_{\min} \rho_{\min}^2 (x^2 - \rho_{\max}^2)^2 \right]^{-\frac{1}{2}}, \quad (\text{B.18})$$

and

$$\widetilde{f}(x, \rho_{\max}, Z) = \left[\frac{Z^2}{4(Z-1)} x^2 (1 - \rho_{\max}^2)^2 - (x^2 - \rho_{\max}^2)^2 \right]^{-\frac{1}{2}}. \quad (\text{B.19})$$

These equations reduce to the expressions for the monodisperse Z-Cone Model in the case of $a=1$.

References

- [1] P. Stevenson, X. Li, *Foam Fractionation: Principles and Process Design*, CRC Press, 2014.
- [2] W.R. Rossen, *Foams in enhanced oil recovery*, in: R.K. Prud'homme, S. Khan (Eds.), *Foams: Theory, Measurements and Applications*, Marcel Dekker, 1996, pp. 413–464.
- [3] K.A. Brakke, The surface evolver, *Exp. Math.* 1 (2) (1992) 141–165.
- [4] A.M. Kraynik, D.A. Reinelt, F. van Swol, Structure of random foam, *Phys. Rev. Lett.* 93 (20) (2004) 208301.
- [5] D. Durian, Foam mechanics at the bubble scale, *Phys. Rev. Lett.* 75 (26) (1995) 4780.
- [6] M. Sexton, M. Möbius, S. Hutzler, Bubble dynamics and rheology in sheared two-dimensional foams, *Soft Matter* 7 (23) (2011) 11252–11258.
- [7] V.J. Langlois, S. Hutzler, D. Weaire, Rheological properties of the soft-disk model of two-dimensional foams, *Phys. Rev. E* 78 (2008) 021401.
- [8] S. Hutzler, R.P. Murtagh, D. Whyte, S.T. Tobin, D. Weaire, Z-cone model for the energy of an ordered foam, *Soft Matter* 10 (36) (2014) 7103–7108.

- [9] D. Morse, T. Witten, Droplet elasticity in weakly compressed emulsions, *Europhys. Lett.* 22 (7) (1993) 549.
- [10] M.-D. Lacasse, G.S. Grest, D. Levine, Deformation of small compressed droplets, *Phys. Rev. E* 54 (5) (1996) 5436.
- [11] D. Weaire, S. Hutzler, *The Physics of Foams*, Clarendon Press, 1999.
- [12] A. Maestro, W. Drenckhan, E. Rio, R. Höhler, Liquid dispersions under gravity: volume fraction profile and osmotic pressure, *Soft Matter* 9 (8) (2013) 2531–2540.
- [13] H. Princen, Osmotic pressure of foams and highly concentrated emulsions: I. Theoretical considerations, *Langmuir* 2 (4) (1986) 519–524.
- [14] H. Princen, S. Friberg, K. Larsson, J. Sjöblom, Structure, mechanics, and rheology of concentrated emulsions and fluid foams, in: *Food emulsions*, 4th ed., CRC Press, 2004, pp. 413–483.
- [15] R. Höhler, Y. Yip Cheung Sang, E. Lorenceau, S. Cohen-Addad, Osmotic pressure and structures of monodisperse ordered foam, *Langmuir* 24 (2) (2008) 418–425.